Journal of the Serbian Society for Computational Mechanics / Vol. 16 / No. 1, 2022 / pp 85-108
(10.24874/jsscm.2022.16.01.07)

EFFECT OF VERTICAL POSITION OF HEATED SQUARE OBSTACLE ON NATURAL CONVECTION IN POROUS CAVITIES SATURATED BY A NANOFLUID USING BUONGIORNO'S TWO PHASE MODEL

Fatima-Z Khelif[1*], Mustapha Helmaoui[1], Mohamed Bouzit[1], Abderrahim Mokhefi[2]

[1] Faculty of Mechanical Engineering, University of Science and Technology of Oran, Mohamed Boudiaf, El Mnaouar, BP 1505, Bir El Djir 31000, Oran, Algeria
e-mail: kheliffatimaz@gmail.com, helmaouisara@yahoo.fr, bouzit_mohamed@yahoo.fr
[2] Faculty of Sciences and Technology, Bechar University B.P.417, 08000, Bechar, Algeria
e-mail: abderrahim.mokhefi@univ-bechar.dz
**corresponding author*

Abstract

Laminar flow, heat transfer and mass transfer of nanofluid in a porous medium have been studied using Buongiorno's two phase model. The porous medium in place is a non-uniform octagonal shape. In order to increase the rate of heat transfer within the porous cavity, it has been equipped with a heated square at different vertical positions from position 1 (P1) to position 5 (P5). The left wall of this cavity is maintained at a high temperature and a unit volume fraction; whereas the right wall is exposed to a low temperature and a canceled volume fraction, and the other walls have been assumed to be adiabatic. The purpose of this paper is to highlight the effect of the heated square at different vertical positions on the evolution of the hydrodynamic, thermal and mass profiles taking into account the influence of certain parameters, such as: Rayleigh number ($10^2 \leq Ra \leq 10^4$), Darcy number ($10^{-6} \leq Da \leq 10^{-2}$), thermophoresis ratio ($0.1 \leq Nt \leq 1$), buoyancy ratio ($0.1 \leq Nr \leq 1$), Brownian motion ratio ($0.1 \leq Nb \leq 1$) and Lewis number ($0.1 \leq Le \leq 1$). The physical phenomenon studied is governed by the Navier-Stokes equations coupled with the energy equation and the mass conservation equation (continuity of nanoparticles). These differential equations of boundary conditions are solved using the finite element method. The results show that an increase in the Rayleigh number and the Darcy number improves natural convection, leading to an increase in the Nusselt number at the square. It is also found that the lowest values of the Nusselt number are located at the extremities of the cavity while the highest are located at the intermediate position between the positions P3 and P4 regardless of the values of the different parameters. On the other hand, an increase in the Darcy number leads to an increase in the vertical and horizontal velocity where the highest values are located at position P4.

Keywords: Natural convection, porous medium, Buongiorno's Model, nanofluids.

1. Introduction

Thermal fluids are very important for heat transfer so an innovative technique consists in using nanofluids and because of its unique structure the porous medium has been the subject of several investigations. Recently, natural convection in open enclosure and saturated porous medium has generated a great deal of interest due to its applications in areas such as solar energy storage, electronic cooling devices, buildings, etc. The researchers are, therefore, more concentrated on nanofluids because of their high thermal conductivity. Izadi M. et al. (2018), Alsabery A.I et al. (2018) and Motlagh S. and Motlagh M. (2017) studied natural convection of nanofluid using Buongiorno's two phase model, while Sheremet M. et al. (2017), Sheremet M.A. et al. (2015), Ahmed Sameh E. and Rashed Z.Z. (2019) and Bhowmick D. et al. (2021) studied free convection in porous wavy cavities using Buongiorno's nanofluid model. Oztop H. F. (2006) and Alsabery A. et al. (2018) investigates mixed convection in a porous lid-driven enclosure. Motlagh S. et al. (2016) and Sheremet M. and Pop I. (2018) inspected natural convection in an inclined porous nanofluid cavity using Buongiorno's mathematical model. Hussain S. and Ahmed S. (2019), Hoghoughi G. et al. (2018), Sheremet M. et al. (2015 a), Sheremet M.A. et al. (2015 b), Tham L. et al. (2014) treated the natural convection of nanofluid with porous materials using Buongiorno's mathematical model. Mustafa M. (2017) analyzed a flow of nanofluids in the presence of a magnetic field given the Buongiorno model. The results obtained by Alsabery A.I. et al. (2020) show that the porosity increases the average Nusselt number at a higher Darcy number while its influence remains negligible at a low Darcy number. Hu P. and Li Q. (2020) found that partially filled porous systems with internal heat source on forced convection have better thermal characteristics. Chu Y. et al. (2021) reported that velocity decreases with an increase in magnetic parameter. The thermal field and associated layer thickness is more subject to larger Brownian motion and thermophoresis parameters. Sheikhzadeh A. and Nazari S. (2013) found that heat transfer increases with the increase in both Rayleigh number and Darcy number. It is further observed that the heat transfer in the cavity is improved by increasing of solid volume fraction parameter of nanofluids. Sheremet M. A. et al. (2017) treated the effect of Rayleigh, Lewis number and buoyancy-ration on fluid flow, heat and mass transfer in two entrapped triangular cavities filled with nanofluid using the Buongiorno model. Lahlou S. et al. (2020) studied the flow of viscoplastic fluids filled with hybrid nanoparticles and found that the distribution of particles is the same for both constituents. Chandra Sekhar Reddy R. and Sudarsana Reddy P. (2020) showed that, in steady and unsteady cases, by increasing the wedge angle value the temperature of the liquid increases. Aldabesh A. et al. (2021) adopted the Buongiorno model to study the Brownian effect and the thermophoresis diffusion parameters and found that when the Reynolds and Prandtl numbers increase, the temperature profile decreases. Mahanthesha B. et al. (2021) demonstrated that two heat source mechanisms conduct to improve the temperature profile and the Brownian parameter is sensitive to the heat transfer. The numerical study in Chen H. et al. (2021) indicates that the baffles with porous blocks and the aerodynamic baffles increase the performance of the cell. Ahmad R. et al. (2017) concluded that the Brownian diffusion does not change the rate of heat transfer to the needle surface and the maximum heat transfer rate is achieved for the situation in which the thermophoresis effect is absent. In the study by Lakshmi K.M. et al. (2020), the results of the KVL single-phase model are obtained by taking the nanoparticles concentration value to be zero. Ali B. et al. (2021) noticed that high values for thermophoresis, shape factors, Brownian motion and volume fraction significantly improved temperature, also computing Nusselt number and Sherwood number allow to expose the physical aspect of this study. Zhang Y. et al. (2022) focused on the field synergy theory and concluded that the porous cooling channel had a higher heat transfer coefficient, which improved the PV/T system.

The present paper deals with the natural convection in open cavities filled with porous medium equipped with a hot square using Buongiorno's two phase nanofluid model and it

consists of five sections. It begins with an introduction, where the previous research carried out in the field is reviewed. In section 2, the fundamental equations governing the problem and the boundary conditions are mentioned. In section 3, the proposed physical geometry, the validation results and the results found in the literature are presented, and a mesh study is carried out. In section 4, computational simulation results that show the influence of the several parameters on the nanofluid flow is discussed. Finally, section 5represents an overall conclusion summarizing the main results obtained in the paper.

2. Fundamental relations

2.1 Governing equations

The dimensional equations which govern laminar flow in a porous medium are the conservation of momentum (Navier-Stokes), energy (heat) and dispersion (concentration: Buongiorno)

$$\frac{\partial u}{\partial x}+\frac{\partial v}{\partial y}=0 \tag{1}$$

$$\rho\left(u\frac{\partial u}{\partial x}+v\frac{\partial u}{\partial y}\right)=-\frac{\partial P}{\partial x}+\mu\left(\frac{\partial^2 u}{\partial x^2}+\frac{\partial^2 u}{\partial y^2}\right)-\frac{\mu}{K}u \tag{2}$$

$$\begin{aligned}&\rho\left(u\frac{\partial u}{\partial x}+v\frac{\partial u}{\partial y}\right)=-\frac{\partial P}{\partial y}+\mu\left(\frac{\partial^2 v}{\partial x^2}+\frac{\partial^2 v}{\partial y^2}\right)-\frac{\mu}{K}v\\&+\left[\left(1-C_c\right)\rho_f\left(T-T_c\right)\beta_f-\left(C-C_c\right)\left(\rho_S-\rho_f\right)\right]g\end{aligned} \tag{3}$$

$$\begin{aligned}&u\frac{\partial T}{\partial x}+v\frac{\partial T}{\partial y}=\alpha\left(\frac{\partial^2 T}{\partial x^2}+\frac{\partial^2 T}{\partial y^2}\right)\\&+\delta\left\{D_B\left(\frac{\partial T}{\partial x}\frac{\partial C}{\partial x}+\frac{\partial T}{\partial y}\frac{\partial C}{\partial y}\right)+\frac{D_T}{D_c}\left[\left(\frac{\partial T}{\partial x}\right)^2+\left(\frac{\partial T}{\partial Y}\right)^2\right]\right\}\end{aligned} \tag{4}$$

$$u\frac{\partial C}{\partial x}+v\frac{\partial C}{\partial y}=D_B\left[\left(\frac{\partial^2 C}{\partial x^2}+\frac{\partial^2 C}{\partial y^2}\right)+\frac{D_T}{D_c}\left(\frac{\partial^2 T}{\partial x^2}+\frac{\partial^2 T}{\partial y^2}\right)\right] \tag{5}$$

Where D_B and D_T are, respectively, the Brownian motion and thermophoresis coefficient. They are defined by $D_B = K_b\, T_0 / 3\pi\, d_p \mu$ and $D_T = \beta\mu C_0 / \rho_f$, respectively, α is the effective thermal conductivity, and the parameter is defined by $\delta = (\rho C_P)_s / (\rho C_P)_f$.

To generalize the studied phenomenon, a set of dimensionless variables has been introduced. It is defined as follows: $X=x / H$, $Y=y / H$, $U=u\, H / \alpha_f$, $V=v\, H / \alpha_f$, $\Theta=(T - T_c) / (T_h - T_c)$, $\phi=C - C_c / C_h - C_c$, $Ra=(1 - C_c)\, \beta_f\, g\, (T_h - T_c)\, H^3 / \nu_f\, \alpha_f$, $Pr=\nu_f / \alpha_f$, $L=\alpha_f / D_B$, $P=p\, H^2 / \rho_f\ \alpha^2_f$, $Nr=(C_h - C_c)(\rho_s - \rho_f) / (1 - C_c)\, \beta_f\, \rho_f\, (T_h - T_c)$, $Da=K / H^2$, $Nb=(C_h - C_c)\, D_B\, (\rho\, C_p)_s / \alpha_f\, (\rho\, C_p)_f = D_B\, \delta\, (C_h - C_c) / \alpha_f$, $Nt=D_T\, (\rho\, C_p)_s\, (T_h - T_c) / T_c\, (\rho\, C_p)_f\, \alpha_f = D_T\, \delta\, (T_h - T_c) / T_c\, \alpha_f$.

$$\frac{\partial U}{\partial X}+\frac{\partial V}{\partial Y}=0 \tag{6}$$

$$U\frac{\partial U}{\partial X}+V\frac{\partial U}{\partial Y}=-\frac{\partial P}{\partial X}+Pr\left(\frac{\partial^2 U}{\partial X^2}+\frac{\partial^2 U}{\partial Y^2}\right)-\frac{Pr}{Da}U \tag{7}$$

$$U\frac{\partial V}{\partial X}+V\frac{\partial V}{\partial Y}=-\frac{\partial P}{\partial Y}+Pr\left(\frac{\partial^2 V}{\partial X^2}+\frac{\partial^2 V}{\partial Y^2}\right)-\frac{\mathrm{Pr}}{Da}V+Ra\ Pr\left(\theta-Nr\phi\right) \tag{8}$$

$$U\frac{\partial \theta}{\partial X}+V\frac{\partial \theta}{\partial Y}=\left(\frac{\partial^2 \theta}{\partial X^2}+\frac{\partial^2 \theta}{\partial Y^2}\right)+Nb\left(\frac{\partial \theta}{\partial X}\frac{\partial \phi}{\partial X}+\frac{\partial \theta}{\partial Y}\frac{\partial \phi}{\partial Y}\right)+Nt\left[\left(\frac{\partial \theta}{\partial X}\right)^2+\left(\frac{\partial \theta}{\partial Y}\right)^2\right] \tag{9}$$

$$\frac{\partial \phi}{\partial X}+V\frac{\partial \phi}{\partial Y}=\frac{1}{L}\left(\frac{\partial^2 \phi}{\partial X^2}+\frac{\partial^2 \phi}{\partial Y^2}\right)+\frac{Nt}{Nb}\left[\frac{\partial^2 \theta}{\partial X^2}+\frac{\partial^2 \theta}{\partial Y^2}\right] \tag{10}$$

2.2 Boundary conditions

The proposed problem is subjected to the following boundary conditions in the dimensionless form of the cavity walls:

- On the left wall of the cavity: $U=0,\quad V=0,\quad \Theta=1,\quad \phi=1.$
- On the right wall of the domain: $\partial U/\partial X=0,\quad \partial V/\partial X=0,\quad \Theta=1,\quad \phi=1.$
- On the top wall of the domain: $\partial U/\partial Y=0,\quad \partial V/\partial Y=0,\quad \partial \Theta/\partial Y=0,\quad \partial \phi/\partial Y=0.$
- On the bottom wall of the domain: $\partial U/\partial Y=0,\quad V=0,\quad \partial \Theta/\partial Y=0,\quad \partial \phi/\partial Y=0.$

No-slip conditions for the velocity a homogeneous flow for temperature and concentration was defined over all the walls remain.

2.3 Nusselt number

To analyse the heat transfer characteristics, the Nusselt is one of the most important dimensionless quantity variables. It is used to compare the rate of the heat transfer by convection and conduction, and it is given by

$$Nu=\frac{hW}{k} \tag{11}$$

where h is the coefficient of heat transfer and it is given by

$$h=\frac{q}{T_h-T_c} \tag{12}$$

where q is the heat flux at the wall

$$q=-k\frac{\left(T_h-T_c\right)}{W}\frac{\partial \theta}{\partial X}\bigg|_{X=0} \tag{13}$$

$$Nu=-\frac{\partial \theta}{\partial X}\bigg|_{X=0} \tag{14}$$

$$Nu_{avg}=\frac{1}{L_s}\int_0^{L_s} Nu\ ds \tag{15}$$

where L_S is the total length of the wall.

2.4 Nomenclature

k	Thermal conduction ($Wm^{-1}K^{-1}$)
g	Gravitational acceleration ($m\ s^{-1}$)
C_p	Specific heat ($J\ kg^{-1}K^{-1}$)
Pr	Prandtl number
Nu	Nusselt number (local)
Ra	Rayleigh number
Da	Darcy number
Nr	Buoyancy ratio number
Nb	Brownian motion parameter
L	Lewis number
Nt	thermophoresis parameter
Nu_{avg}	Average Nusselt
x, y	Space coordinates in dimensional form (m)
X, Y	Dimensionless space coordinate
u, v	Velocity components in dimensional form (m^{-1})
p	Pressure (Nm^{-2})
T	Temperature in dimensional form (K)
U, V	Dimensionless velocity components
P	Dimensionless pressure
ν	Kinetic viscosity (m^2s^{-1})
μ	dynamic viscosity ($kg\ m^{-1}s^{-1}$)
β	Thermal expansion coefficient (K^{-1})
ρ	density ($kg\ m^{-3}$)
α	thermal diffusivity ($m^2\ s^{-1}$)
θ	dimensionless temperature
ϕ	dimensionless concentration
c	cold
h	hot
f	fluid
p	nanoparticles
nf	nanofluid

3. Statement of the problem

3.1 Validation

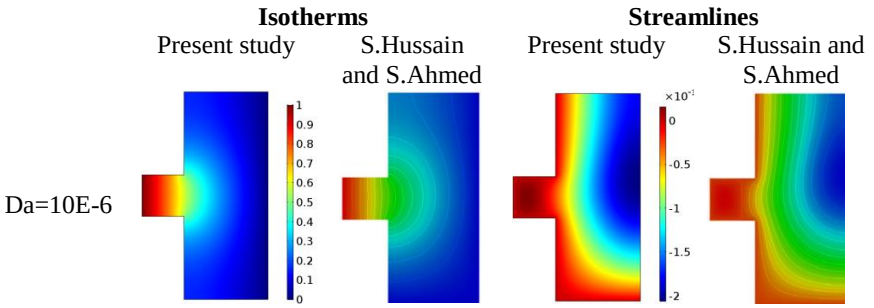

Fig. 1. Comparison of isotherms and streamlines between the reference study and the present study.

The present study has been validated with the results from the work of Hussain Shafqat and Ahmed Sameh E. (2019) for the following parameters: $Ra=10^5$, $Da=10^{-5}$, $Nr=Le=1$, $Nt=Nb=0.5$ and $Pr=6.2$. The validation is done on a porous rectangular open cavity filled with nanofluid varying the Darcy number between 10^{-4} and 10^{-6}. A comparison of the isotherms and streamlines displayed in Fig. 2 shows that the results have practically the same variation.

Another comparison of the average Nusselt number between the reference study and the present study was made. An overall deviation of 2.56 % was obtained for the same conditions as the reference study as shown in Fig. 3.

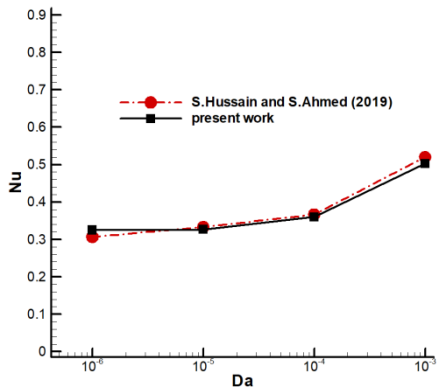

Fig. 2. Average Nusselt number comparison between Hussain S. and Ahmed S. study and the present study.

3.2 Simulation of the new geometry

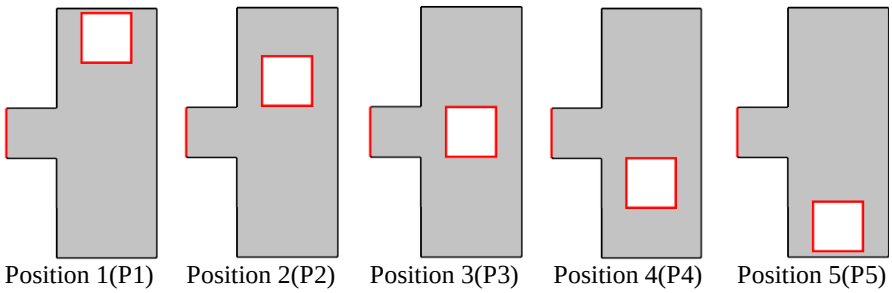

Fig. 3. The new geometry.

A rectangular open cavity filled with a porous medium saturated with nanofluid and a square moving vertically along the height of the rectangle was used to study the natural convection. The cavity has horizontal adiabatic walls, the vertical wall and the square inside are kept to a high constant temperature *Th*, a vertical open face is fixed to a low temperature *Tc* and the vertical walls above and below the aperture are maintained insulated. To obtain and analyse results, some simplifications are taken into account: the nanofluid is Newtonian and incompressible; the influence of the slipping, the effect of thermal radiation and viscous dissipation are supposed neglected; the porosity and permeability of the porous medium are supposed to be uniform, and the flow is laminar.

3.3 Mesh Test

A mesh test was carried out in order to choose the one which will allow obtaining stable results with a minimum of elements and an optimal time. An unstructured mesh composed of triangular and quadrilateral elements was discretized on the computational domain. Five meshes were tested to compare the evolution of average Nusselt (*Nu*), maximum value of the streamlines (Ψ max), temperature (*T*) and concentration (*C*) for: $Ra=10^5$, $Da=10^{-3}$, *Nr=Le=1*, Nt=Nb=0.5 and Pr=6.2 as shown in Table 1. For the current study, we opted for the fourth mesh.

Elements	17720	26986	39170	**65936**	104290
Time	42 s	61 s	91 s	**154 s**	251 s
Ψ max	6.45	4.48	6.49	**6.5**	6.5
T	0.18409	0.18304	0.18251	**0.18188**	0.18154
C	0.20095	0.20023	0.19987	**0.19945**	0.19922

Table 1. Independence mesh test for the present configuration.

4. Results and discussion

Natural convection in a vertical rectangular enclosure in a porous cavity filled with nanofluids was studied numerically using a local thermal equilibrium model. The impact of the vertical positions of the heat square on the natural convection was explored. The numerical results are presented by contours of streamlines, isotherms and the variation the Nusselt number at the heated square for several parameter values at various positions of the square as well as the velocity

components on the vertical and horizontal lines inside the domain for a variation of the Darcy number between 10^{-6} and 10^{-2}.

The dimensionless formatting of the governing equations has resulted in a group of dimensionless parameters including the Darcy number (*Da*), the Rayleigh number (*Ra*) as well as the Prandtl number (*Pr*). The range of considered parameters is as follows: $10^2 \leq Ra \leq 10^4$, $10^{-6} \leq Da \leq 10^{-2}$, Nt=0.1, 0.3, 0.5, 0.7, 1, Nb=0.1, 0.3, 0.5, 0.7, 1, Nr=0.1, 0.3, 0.5, 0.7, 1, Le=0.1, 0.3, 0.5, 0.7, 1, and the Prandtl number is fixed the value of 6.2.

Fig. 4 shows streamlines evolution and isotherms respectively for different values of Rayleigh number $10^2 \leq Ra \leq 10^4$ by moving the hot obstacle vertically from position 1 to position 5 with a regular step of 1 (P1, P2, P3, P4, P5) with Nt=Nb=0.5, Nr=1, Le=1, Da=10^{-3} and Pr=6.2. The streamlines evolve from the cold wall on the right to the hot wall on the left (clockwise) skirting the square regardless of the Ra value or the position of the square. High convective transport by raising the value of the Rayleigh number and therefore a high thermal transfer in the cavity is obtained. The modulus of streamlines is more important near the vertical walls of the square. The natural convection increases by increasing Rayleigh and is more significant when the square is in bottom, namely, position 4 (P4) and position 5 (P5). The isotherms are more important in the inferior positions of the hot square (P5, P4 and P3), a symmetric distribution of the isotherms when the hot square is at the center of the cavity (P3) for the low values of Ra which is due to the force of buoyancy.

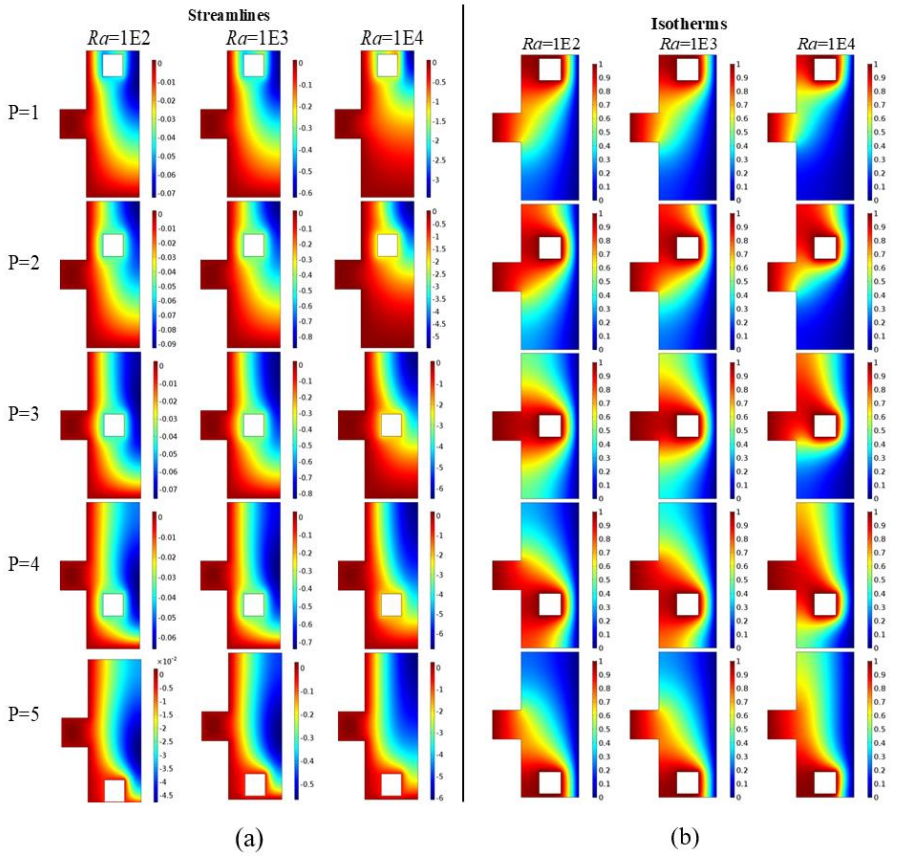

Fig. 4. Impact of vertical position on streamlines (a) and isotherms (b) for natural convection in an open cavity varying *Ra* for Nt=Nb =0.5, Nr=1, Le=1, Ra=1E4, Pr=6.2.

Fig. 5 and Fig. 6**,** respectively, show streamlines and isotherms by varying Darcy number (*Da*) $10^{-6} \leq Da \leq 10^{-2}$ by moving the obstacle vertically from position 1 (P1) to position 5 (P5) with $Ra=10^4$, $Nt=Nb=0.5$, $Nr=1$, $Le=1$ and $Pr=6.2$. It can be noticed that the Darcy number affects the streamlines and isotherms. The streamlines are clockwise and a homogeneous vortex at the level of the convex part indicates the direction of rotation of the nanofluid due to buoyancy. Symmetrical streamlines for $Da=10^{-4}$ at positions P1, P2 and P3. The streamlines are significant on the right square at P4 and P5 positions for different values of the Darcy number. By increasing *Da* the buoyancy increases because increased permeability allows nanofluids to flow more easily, reducing fluid friction within porous medium which results in a better natural convection. We also note that the buoyancy is more significant in the lower positions (P5, P4 and P3), whatever the variation of the Darcy number is. The isotherms cover the entire surface of the cavity but they are specially gathered from the right part of the square to the prominent part. Also, an increase of the Darcy number causes an improvement of the temperature difference inside the cavity which leads to an increase of the natural convection by reducing the resistance force to the flow of the nanofluid in the porous medium.

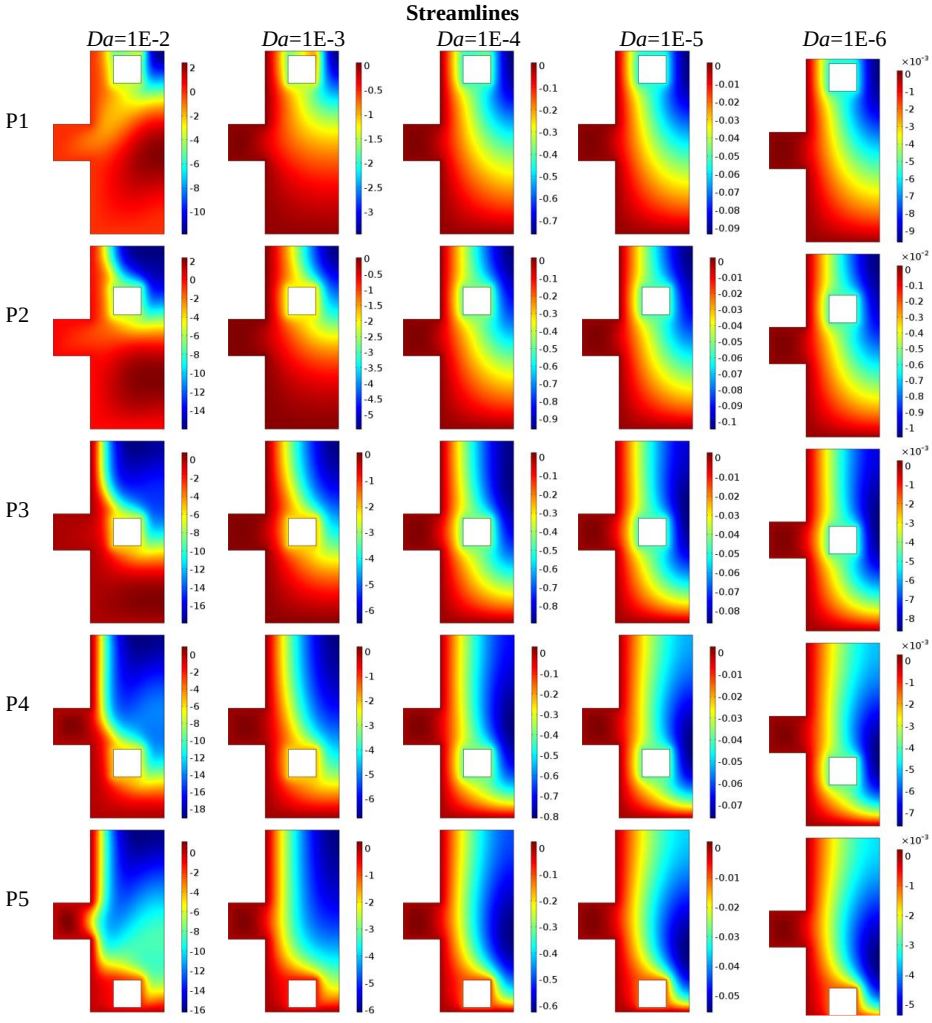

Fig. 5. Impact of vertical position on streamlines for natural convection in an open cavity varying Da for Nt=Nb=0.5, Nr=1, Le=1, Ra=1E4, Pr=6.2.

Fig. 7 and Fig. 8 set out streamlines and isotherms with the variation of bouncy ratio number (*Nr*) $0.1 \leq Nr \leq 1$, $Ra=10^4$, $Da=10^{-3}$, $Nt=Nb=0.5$, $Le=1$, and $Pr=6.2$. The streamlines follow the geometry of the cavity from the right wall at the bottom in a clockwise direction. As the (*Nr*) rises, the strength of the streamlines is reduced, causing a strong natural convection. The isotherms are located at the prominent part and around the square (hot walls) when it is in a higher position (P1, P2), but when it is in a lower position (P3, P4, P5) the isotherms are concentrated between the square and the left wall as well as inside the prominent part. On the other hand, the isotherms are more significant in positions 5 and 4. However, it can be noticed that *Nr* variation has little influence on the isotherms.

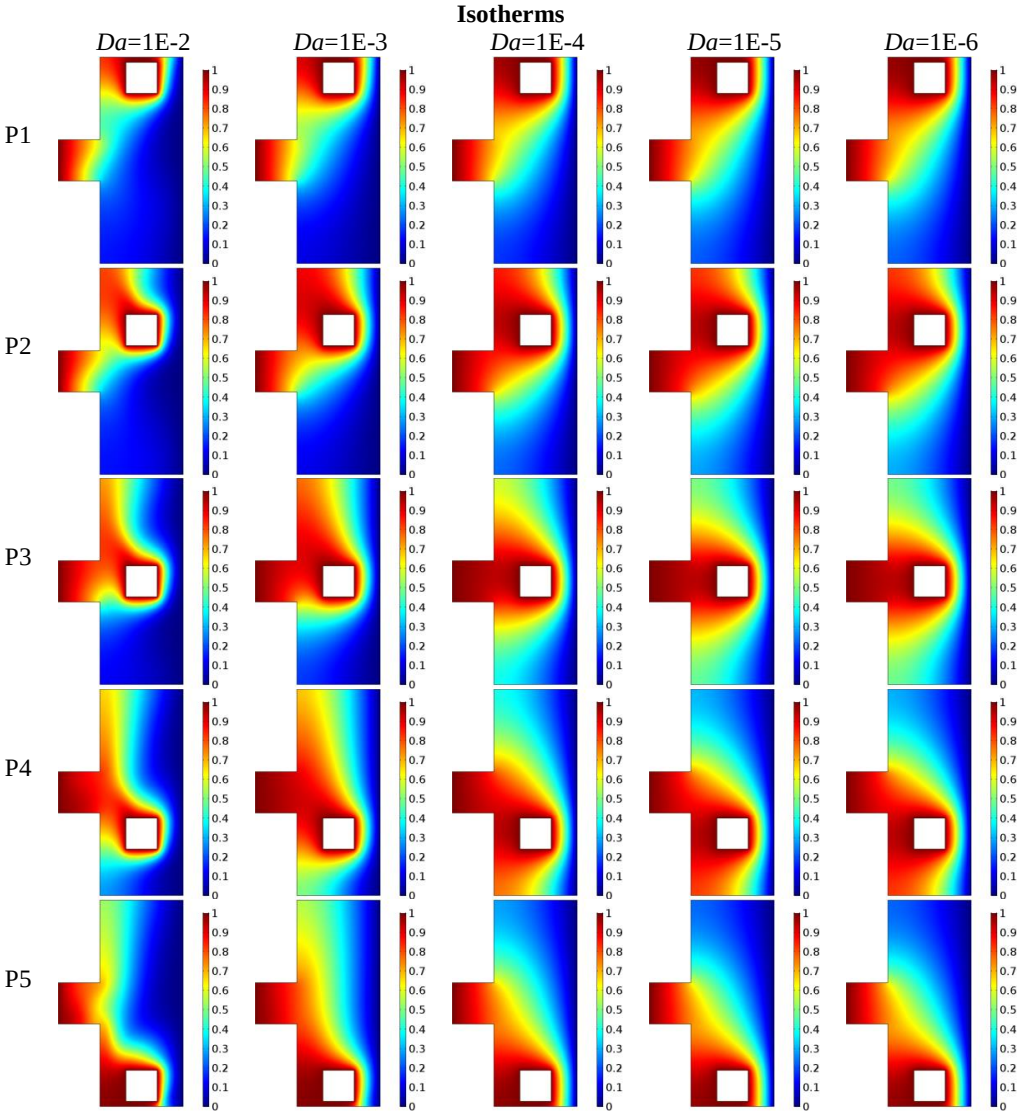

Fig. 6. Impact of vertical position on isotherms for natural convection in an open cavity varying *Da* for *Nt*=*Nb*=0.5, *Nr*=1, *Le*=1, *Ra*=1E4, *Pr*=6.2.

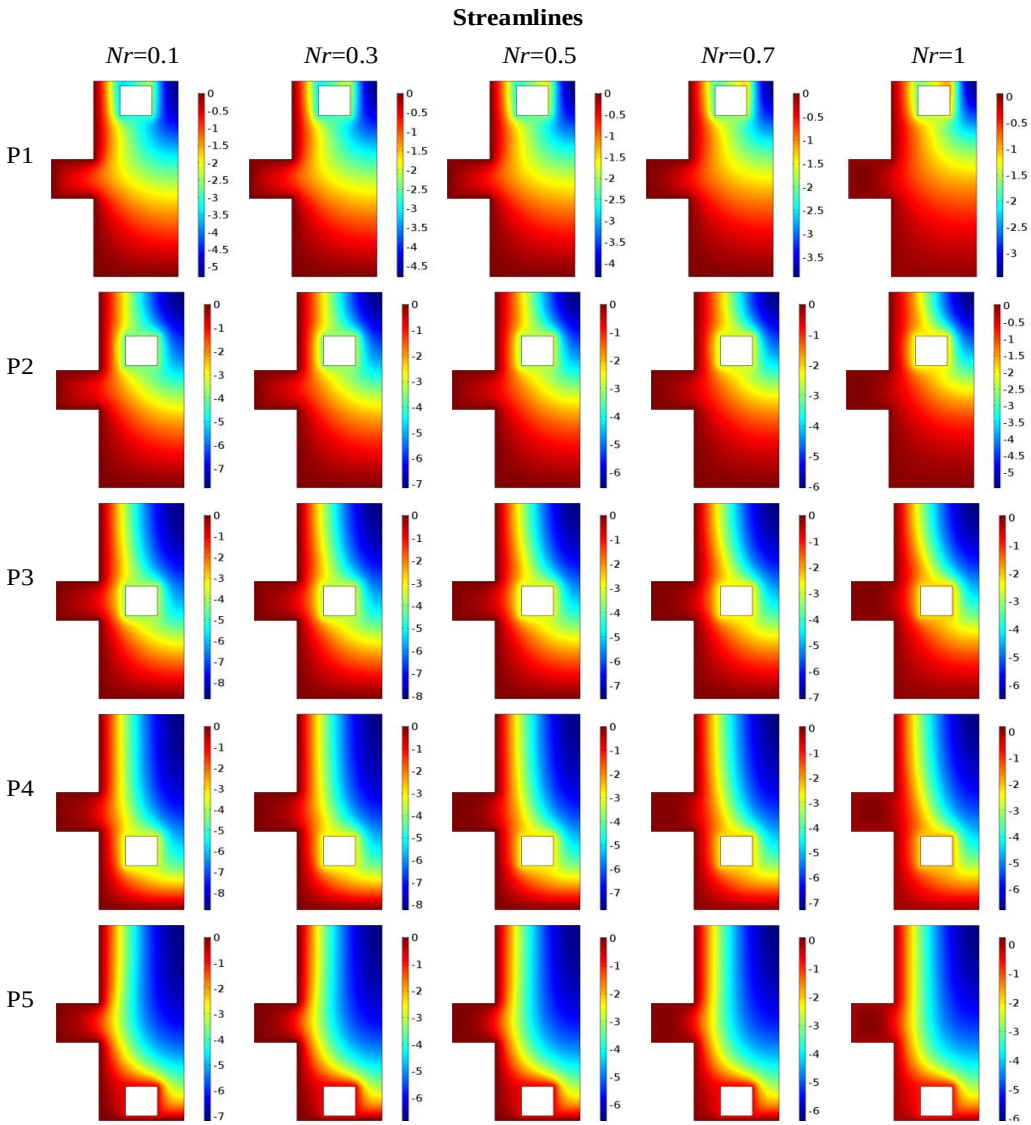

Fig. 7. Impact of vertical position on streamlines for natural convection in an open cavity varying Nr for Nt=Nb=0.5, Da=1E-3, Le=1, Ra=1E4, Pr=6.2.

Fig. 9 and Fig. 10 illustrate variations on streamlines and isotherms, respectively, when changing value of the Lewis number (*Le*) $0.1 \leq Le \leq 1$, $Ra=10^4$, $Da=10^{-3}$, $Nr=1$, $Nt=Nb=0.5$ and $Pr=6.2$. There is a weak impact on the streamlines when the Lewis number *(Le)* is varied. The streamlines are strongest at the external upper corner of the square for all its positions; it is the consequence of a low transfer of the nanoparticles from the high energy zone to the low energy zone. The same comments made on the variation of the isotherms when varying *Le* can be related to the variation of the isotherms when (*Nr*) value changes.

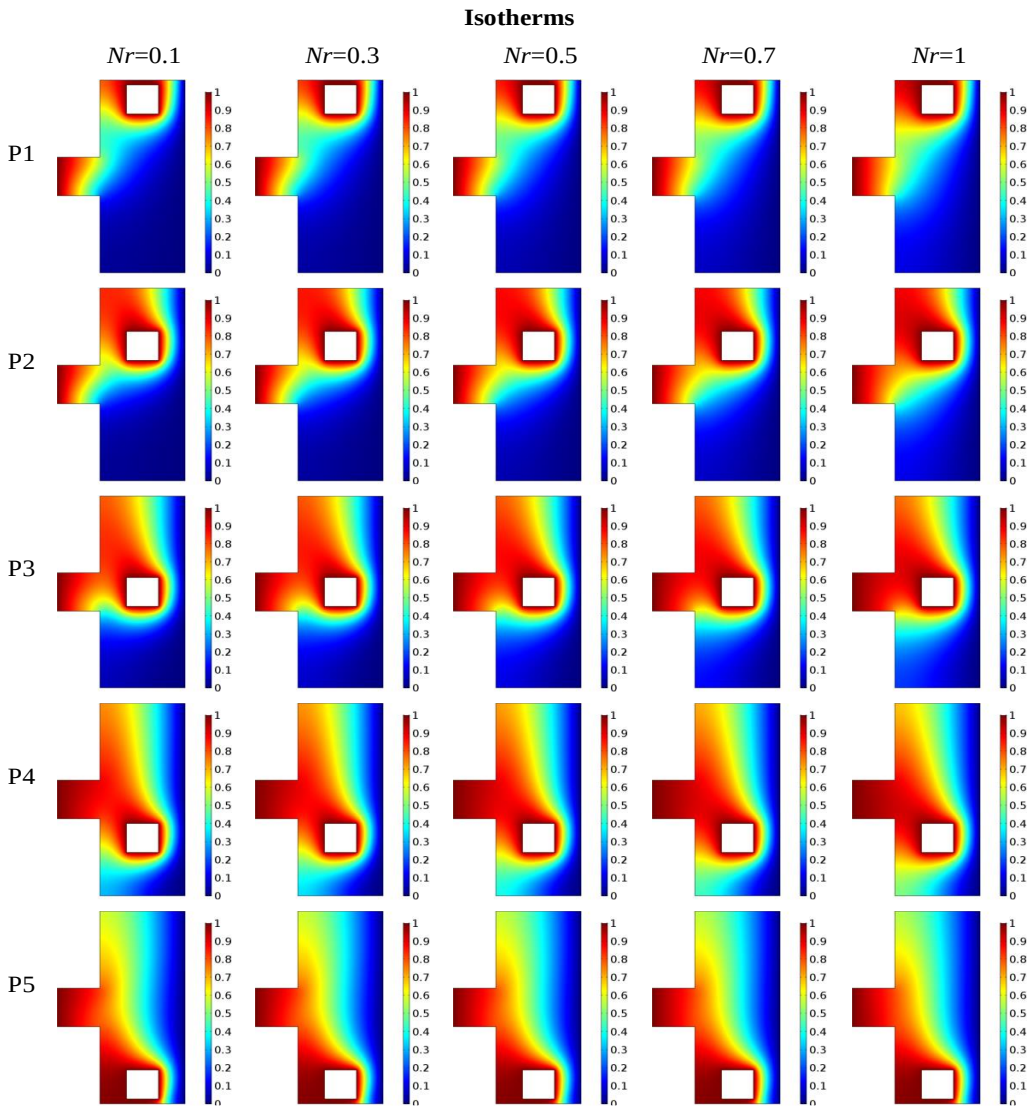

Fig. 8. Impact of vertical position on isotherms for natural convection in an open cavity varying *Nr* for *Nb*=*Nt*=*0.5*, *Le*=1, *Ra*=1E4, *Da*=1E-3, *Pr*=6.2.

Fig. 11 and Fig. 12 show streamlines and isotherms, respectively, with the variation of the Brownian number parameter (*Nb*) $0.1 \leq Nb \leq 1$, $Ra=10^4$, $Da=10^{-3}$, *Le*=1, *Nt*=0.5, *Nr*=1 and *Pr*=6.2. The streamlines modulus increases by increasing the Brownian motion parameter and they are more significant around the square and in low positions. The isotherms are practically the same when the Brownian parameter increases. As observed in the isotherms when varying the *Nr* and the Lewis number, the isotherms are around the square and in the convex part of the cavity for the upper positions of the square. For the lower positions, the isotherms are located between the hot square and the hot wall. As for the two parameters *Nr* and *Le*, a slight influence of the Brownian number on the isotherms is noted.

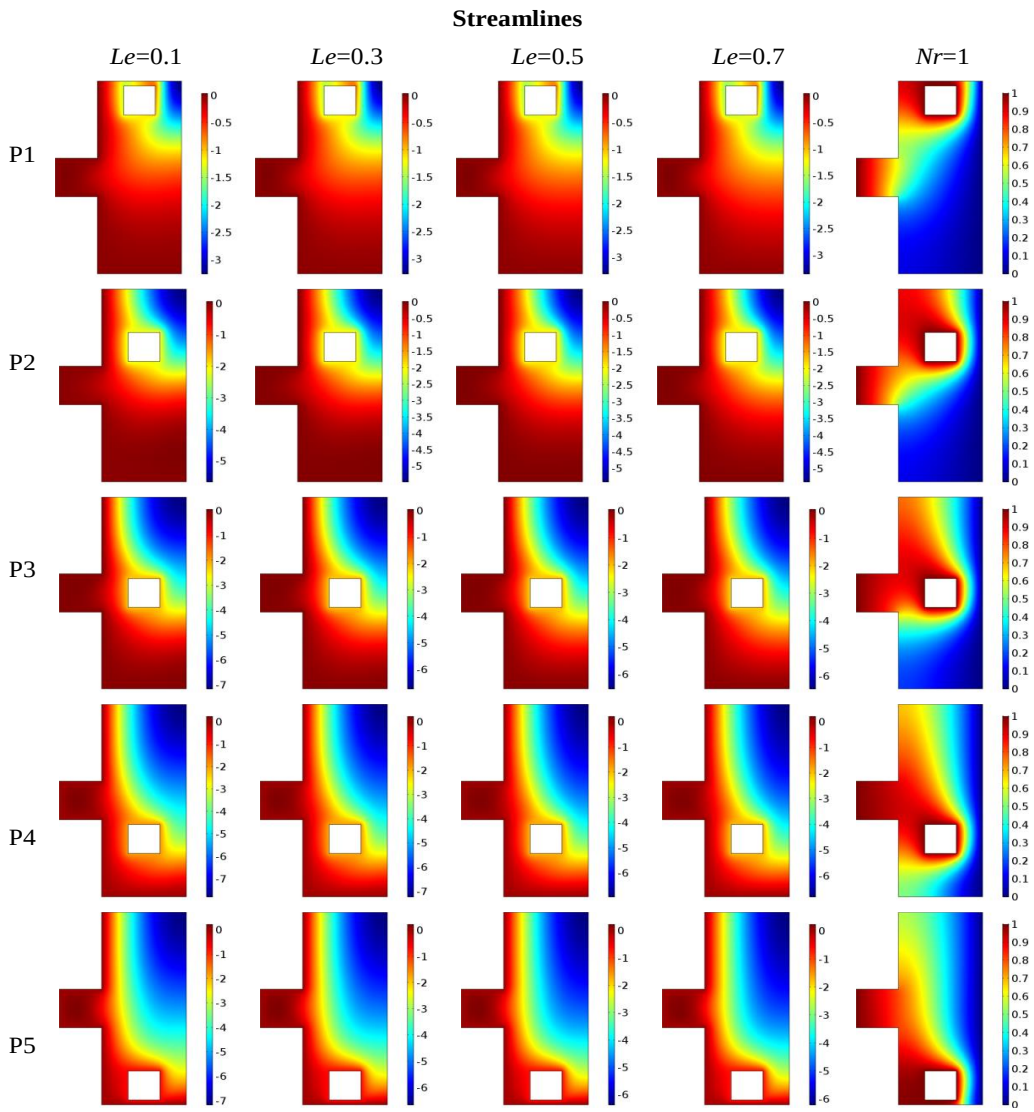

Fig. 9. Impact of vertical position on **s**treamlines for natural convection in an open cavity varying *Le* for *Nt*=*Nb*=*0.5*, *Nr*=1, *Ra*=1E4, *Da*=1E-3, *Pr*=6.2.

Fig. 13 and Fig. 14 display streamlines and isotherms. The thermophoresis number (*Nt*) has the value between 0.1 and 1. The remaining parameters are fixed at $Ra=10^4$, $Da=10^{-3}$, *Nb*=0.5, *Nr*= 1, *Le*=1 and *Pr*=6.2. The variation of the thermophoresis number (*Nr*) has a weak impact on the streamlines. The streamlines move to the cold side (clockwise) where they are more intense. This is due to the displacement of the nanoparticles from the hot side to the cold side as *Nt* increases. By increasing *Nt*, the isotherms are increasing due to a migration of nanoparticles and the nanofluid is made more uniform.

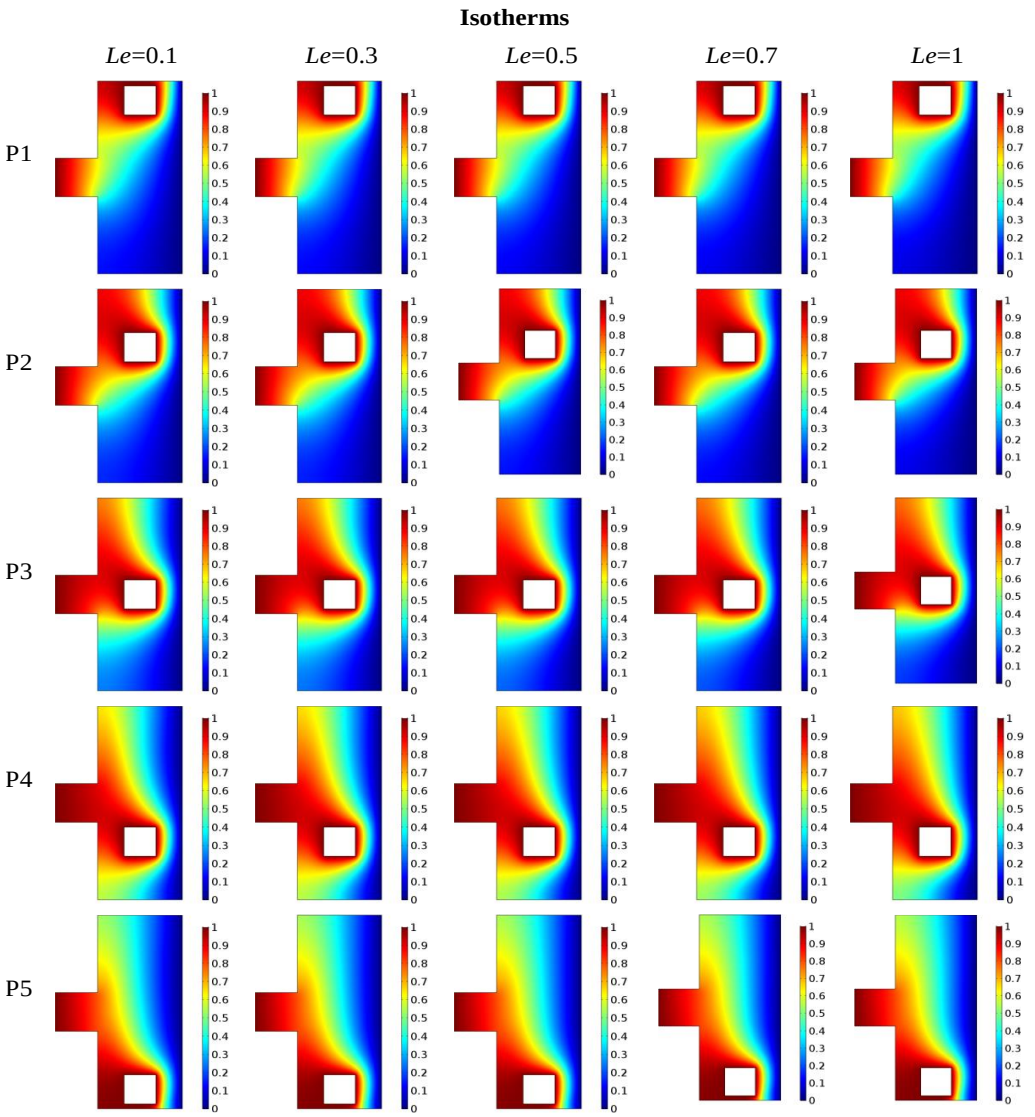

Fig. 10. Impact of vertical position on isotherms for natural convection in an open cavity varying Le for Nt=Nb=0.5, Nr=1, Ra=1E4, Da=1E-3, Pr=6.2.

The observation made on the effects of buoyancy ratio number, Brownian motion parameter and thermophoresis number on the streamlines and isotherms reflects good buoyancy resulting in a good natural convection observed in the inferior positions.

From Fig. 15 to Fig. 19, we can observe the profile of the local Nusselt number at the level of the square at different vertical positions for variations of the Darcy number (*Da*), Rayleigh number (*Ra*), buoyancy ratio number (*Nr*), thermophoresis number (*Nt*), Brownian motion parameter (*Nb*) and Lewis number (*Le*). The obtained results reveal that for all parameters the local Nusselt number increases. The results obtained show that for all parameters, the local Nusselt number is at its minimum value in P5 position and increases as the square moves upwards until the intermediate position between P3 and P4 positions where it starts to decrease. Figures

16, 17 and 19 show that by increasing the Darcy number, the Rayleigh number and the Brownian motion parameter improve the value of the local Nusselt number at the square level. On the contrary, the local Nusselt number increases by reducing the buoyancy ration number and thermophoresis number.

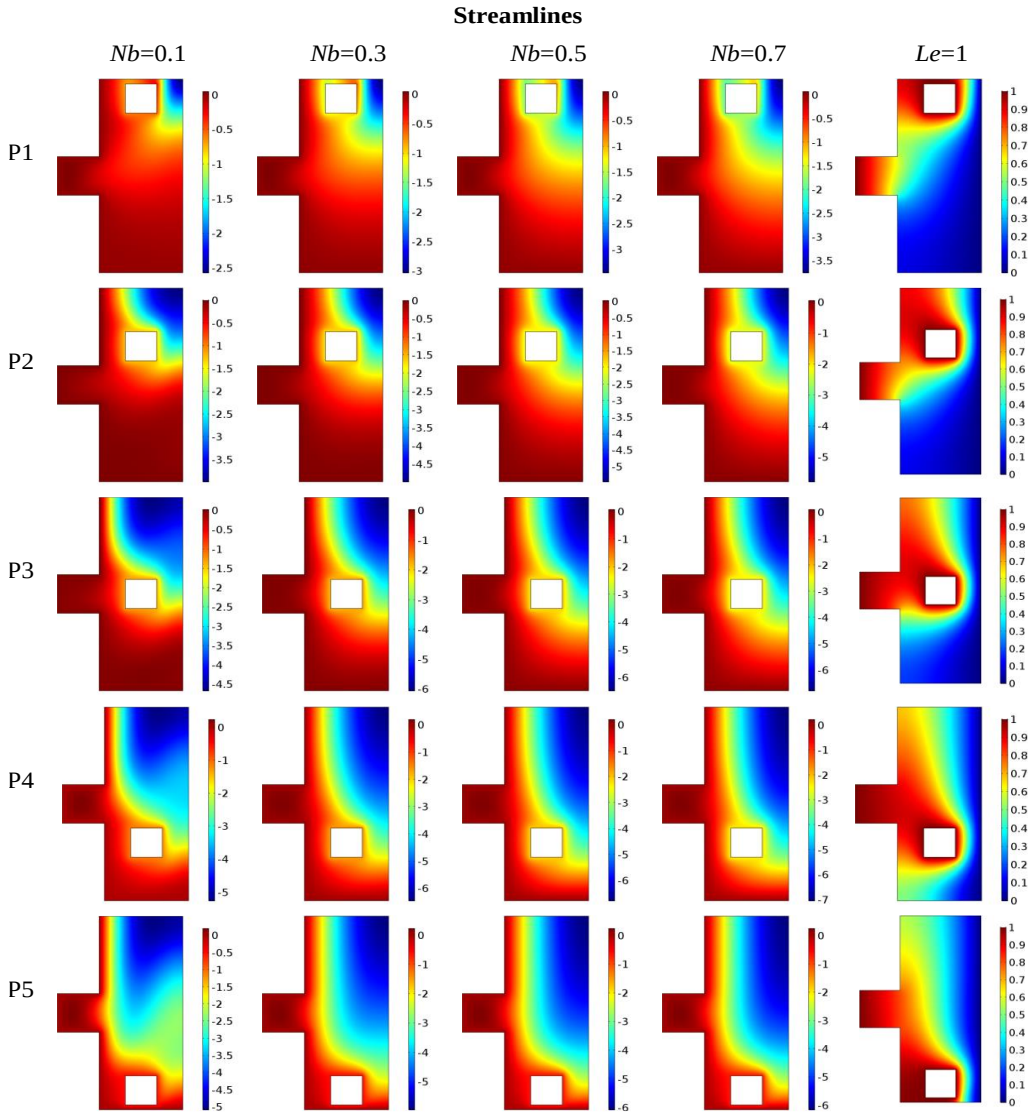

Fig. 11. Impact of vertical position on **s**treamlines for natural convection in an open cavity varying *Nb* for *Nt* =0.5, *Nr*=1, *Le*=1, *Ra*=1E4, *Da*=1E-3, *Pr*=6.2.

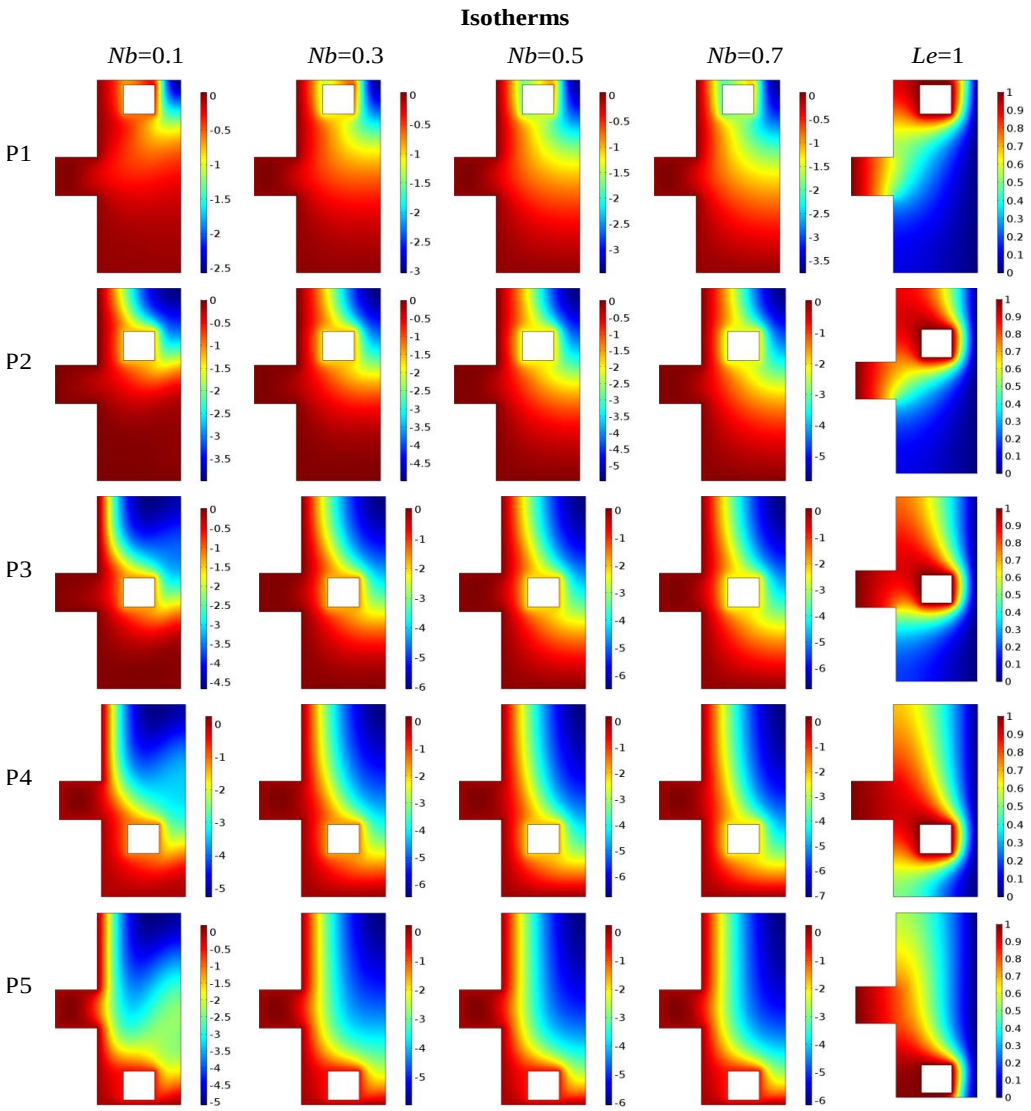

Fig. 12. Impact of the vertical position on isotherms for natural convection in an open cavity varying *Nb* for *Nt =0.5*, *Nr=1*, *Le*=1, *Ra*=1E4, *Da*=1E-3, *Pr*=6.2.

Fig. 20 (a) and (b) displays the effect of the Darcy number on horizontal (u) and vertical velocity (v) along the axis y, respectively, at different verticals positions of the square for parameters mentioned in Fig. 6**.** It shows that by increasing the Darcy number, the vertical and horizontal velocity increase as well. The vertical speed is infinitely small before reaching the different positions of the square. However, it increases and reaches its maximum when approaching the square, and then slightly decreases as the flow passes through the square, after which it slightly increases before decreasing again for $10^{-6} \leq Da \leq 10^{-4}$ where the position 4 represents the highest vertical velocity. For $Da=10^{-3}$ and 10^{-2}, the vertical velocity has the same profile but it increases after the flux passes the square. The values are more important especially for 10^{-2} and the highest velocity is at position 3. The horizontal velocity increases by increasing the Darcy number (Da)

and is more important for Da=10^{-3} and 10^{-2}. The highest horizontal velocity is situated at position 4.

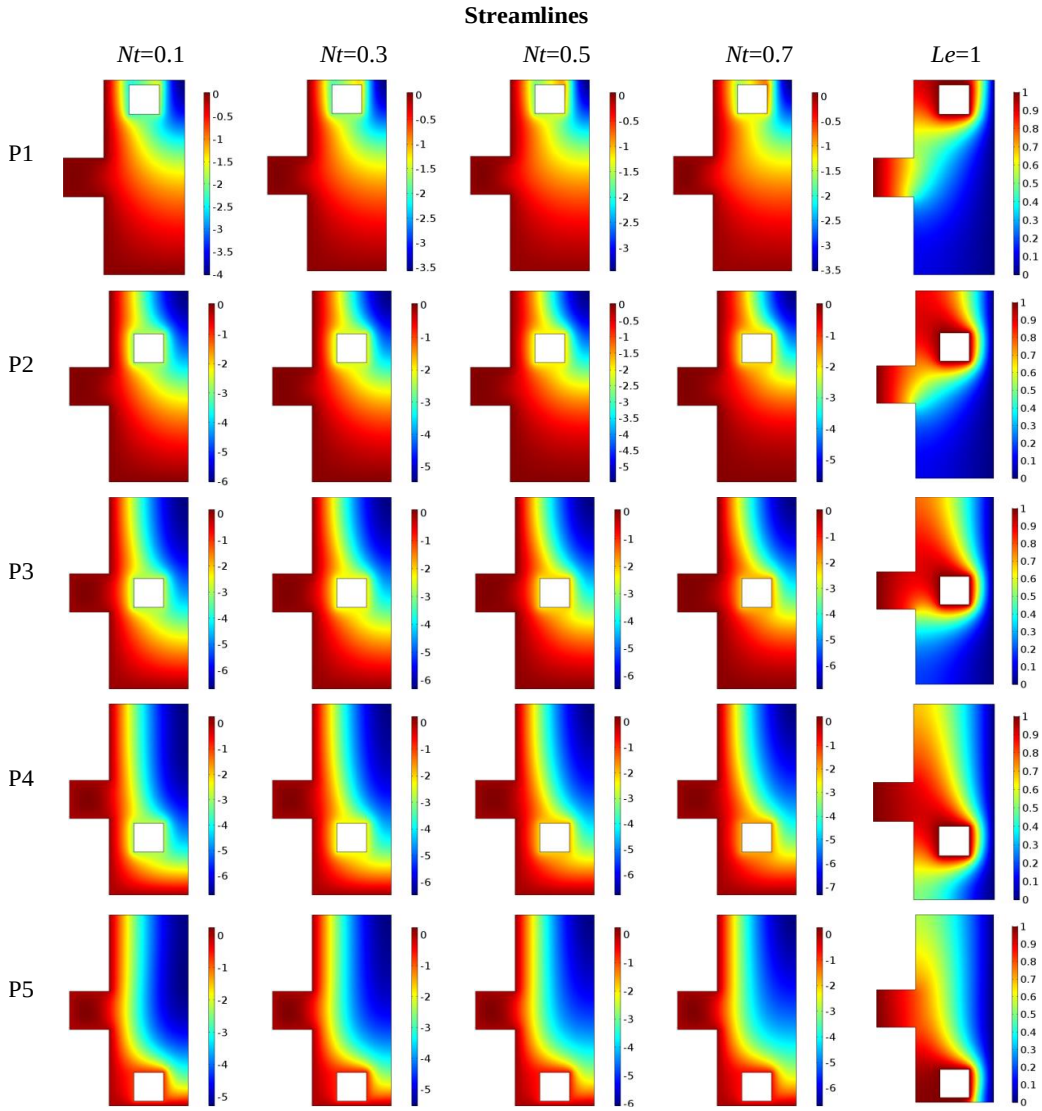

Fig. 13. Impact of vertical position on **s**treamlines for natural convection in an open cavity varying *Nt* for *Nb*=0.5, *Nr*=1, *Le*=1, *Ra*=1E4, *Da*=1E-3, *Pr*=6.2.

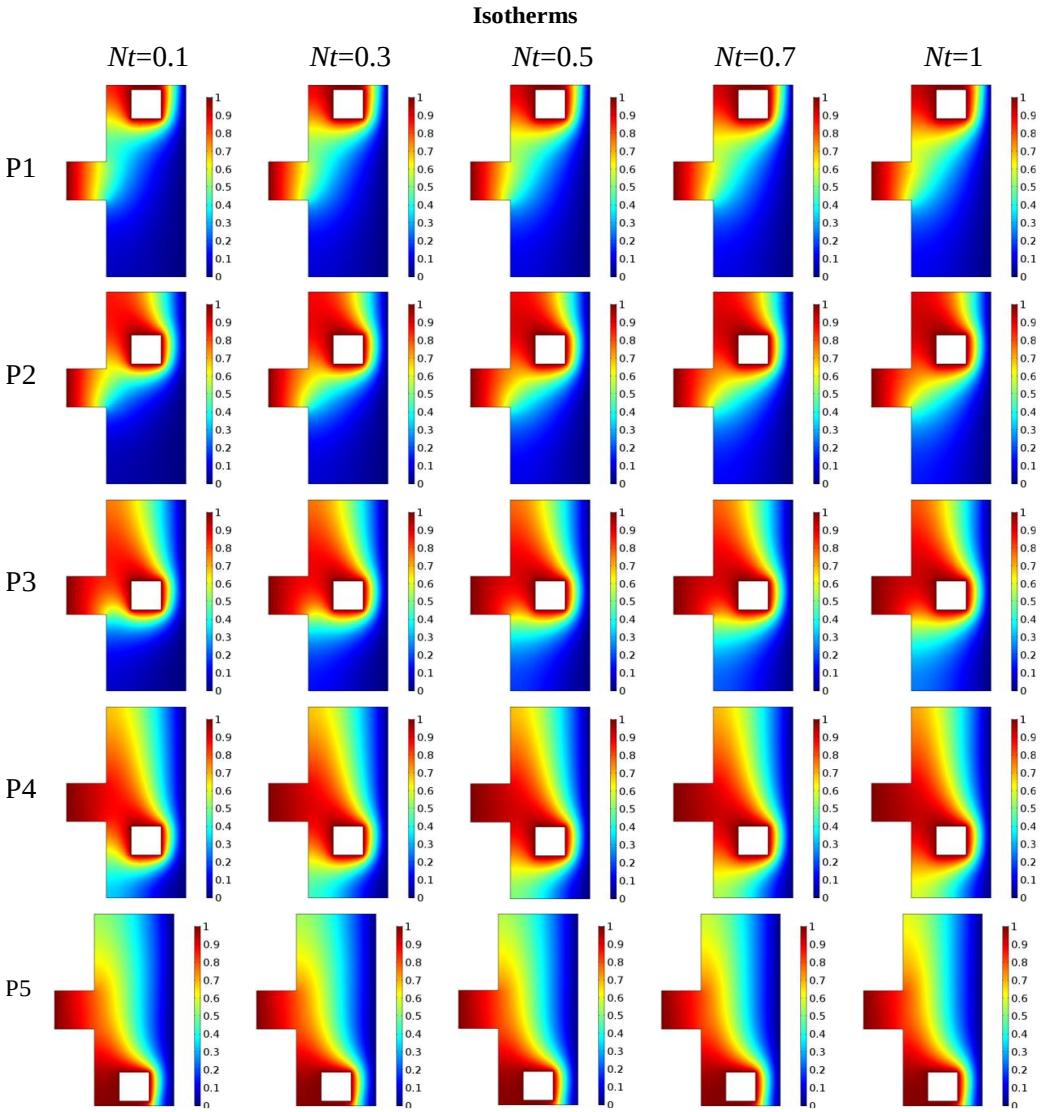

Fig. 14. Impact of vertical position on isotherms for natural convection in an open cavity varying *Nt* for *Nb* =0. , *Nr*=1, *Le*=1, *Ra*=1E4, *Da*=1E-3, *Pr*=6.2.

5. Conclusions

Numerical results obtained to view the impact of the motion of a hot square on the natural heat transfer steady in an open rectangular enclosure saturated with a porous medium filled with nanofluids are presented in this paper. The Darcy model and Buongiorno's model were used to simulate the porous medium and nanofluids, respectively. The transport equations were presented and converted to dimensionless form and then solved numerically using the finite element method. Streamlines, isotherms, local Nusselt number at the heated square as well as the horizontal and vertical velocity were set out for the governing parameters: Rayleigh number,

Darcy number, buoyancy ratio number, Lewis number, Brownian motion parameter and the thermophoresis number. The most important conclusions are as follows:

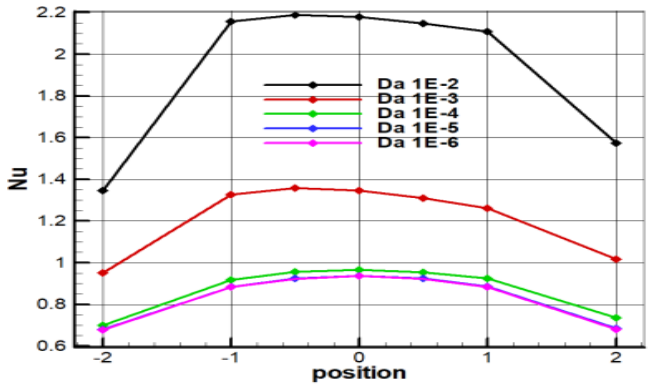

Fig. 15. Nusselt (Nu) at the square by varying the Darcy number according to the position for Nt=Nb=0.5, Nr=1, Le=1, Ra=10^4 and Pr=6.2.

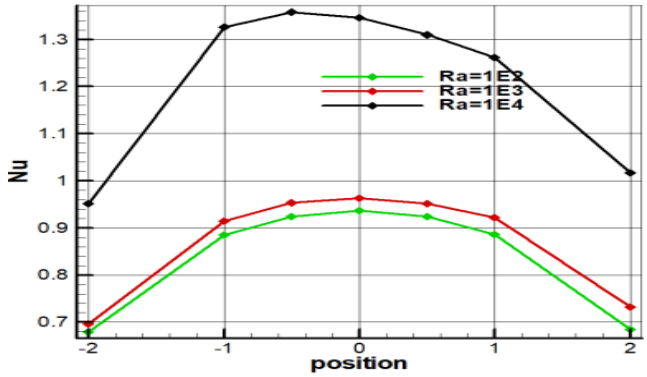

Fig. 16. Nusselt (Nu) at the square by varying the Rayleigh number according to the position for Nt=Nb=0.5, Nr=1, Le=1, Da=10^{-3} and Pr=6.2.

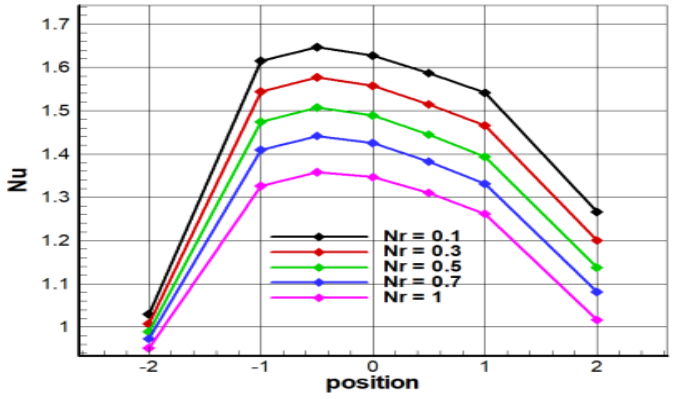

Fig. 17. Nusselt (Nu) at the square by varying the Buoyancy ratio number according to the position for Nt=Nb=0.5, Le=1, Ra=10^4, Da=10^{-3} and Pr=6.2.

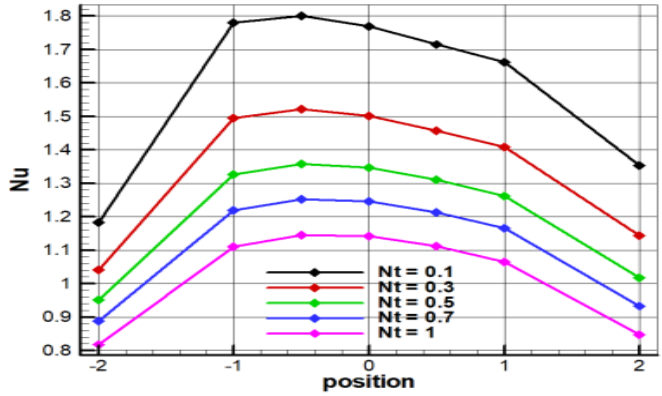

Fig. 18. Nusselt (Nu) at the square by varying the thermophoresis number according to the position for Nr=1, Nb=0.5, Le=1, Ra=10^4, Da=10^{-3} and Pr=6.2.

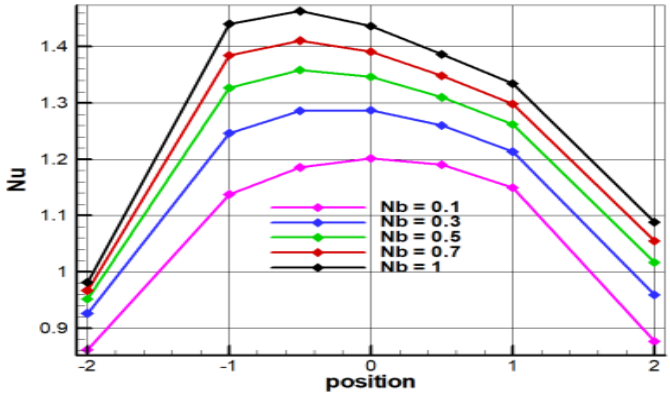

Fig. 19. Nusselt (Nu) at the square by varying the Brownian motion parameter according to the position for Nr=1, Nt=0.5, Le=1, Ra=10^4, Da=10^{-3} and Pr=6.2.

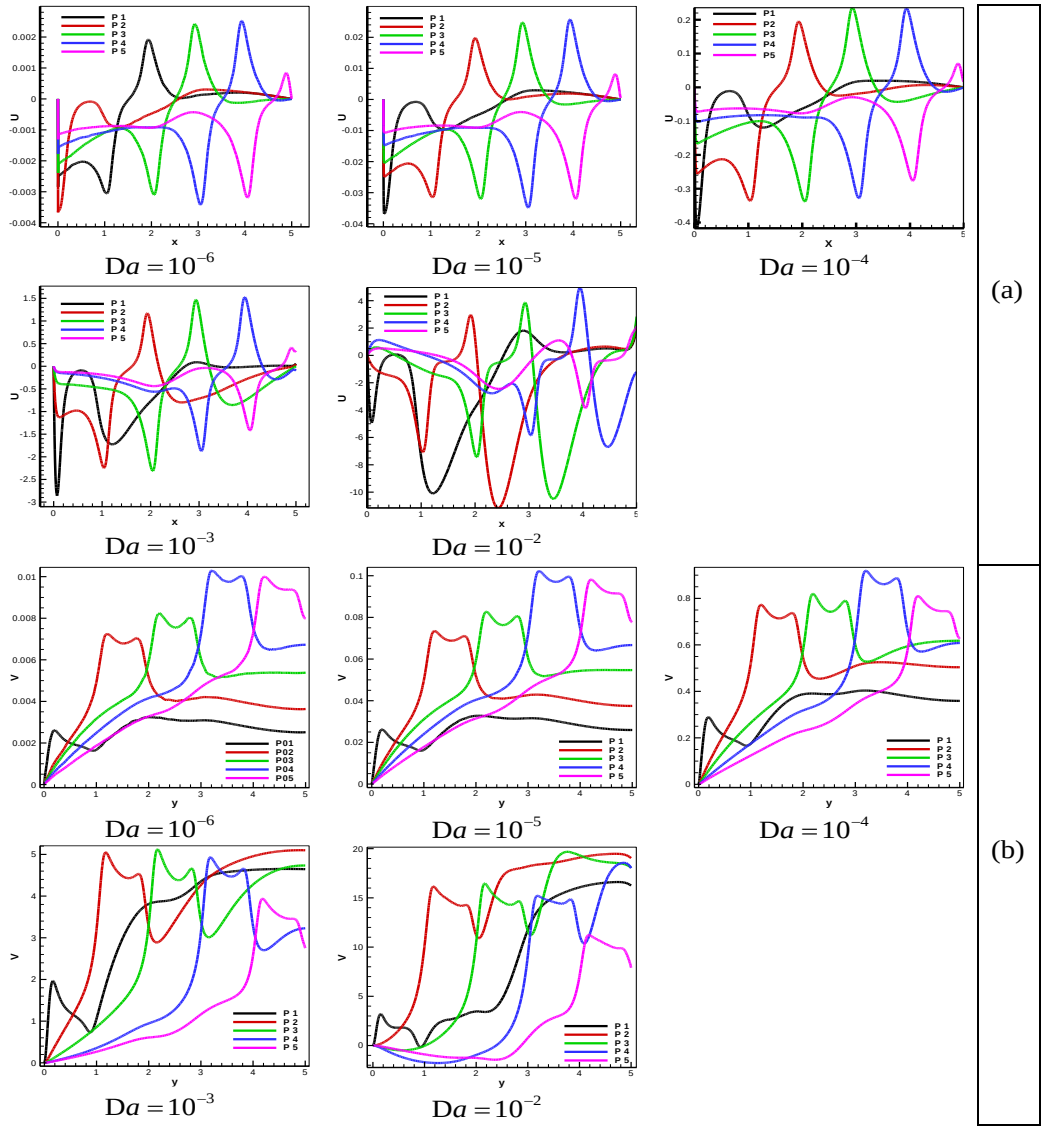

Fig. 20. Darcy number Effect at different positions on (a) Horizontal velocity on the y-axis and (b) Vertical velocity on the y-axis.

- Increase in the Rayleigh number and Darcy number improves natural convection which leads to the increase in the local Nusselt number.
- Increase in the thermophoresis number values and the buoyancy ratio lowers the local Nusselt number.
- Variation of the Lewis number as well as the Brownian motion has little or no influence on natural convection.
- Lowest values of the local Nusselt number are located at the ends of the cavity, i.e. at positions (P1) and (P5).

- Increase in the Darcy number leads to an increase in the vertical and horizontal velocity.
- Highest values of the Nusselt number by varying the various parameters are located at the intermediate position between positions P3 and P4.
- Highest values of the vertical and horizontal velocity are located in position P4.

This study contributes to academic and engineering research because the considered geometry can be used as a passive technique to control the heat transfer. Furthermore, the natural convection in porous media has been an attractive research topic for several authors and remains relevant today due to its various practical applications in different fields such as mechanical engineering including solar heating systems, geothermal energy extraction, oil recovery, heat exchangers and the storage of agricultural products.

References

Ahmad Rida, Mustafaa M., Hina S (2017). Buongiorno's model for fluid flow around a moving thin needle in a flowing nanofluid: A numerical study, Chinese journal of physics 55, 1264-1274.

Ahmed Sameh E., Rashed Z.Z (2019). MHD natural convection in a heat generating porous medium-filled wavy enclosures using Buongiorno's nanofluid model, Case studies in thermal engineering 14, 100430.

Aldabesh A., Hussain Mazmul, Khan Nargis, Riahi Anis, Ullah Khan Sami, Tlili Iskander (2021). Thermal variable conductivity features in Buongiorno nanofluid model between parallel stretching disks: Improving energy system efficiency, Case studies in thermal engineering 23, 100820.

Ali Bagh, Naqvi Rizwan Ali, Ali Liaqat, Abdal Sohaib, Hussain Sajjad (2021). A comparative description on time-dependent rotating magnetic transport of a water base liquid H2O with hybrid nano-materials Al2O3-Cu and Al2O3-TiO2 over an extending sheet using Buongiorno model: Finite element approach, Chinese journal of physics 70, 125-139.

Alsabery A.I., Sheremet M.A., Chamkha A.J., Hashima I (2018). Conjugate natural convection of Al2O3–water nanofluid in a square cavity with a concentric solid insert using Buongiorno's two-phase model, International journal of mechanical sciences 136, 200-219.

Alsabery Ammar I., Ismael Muneer A., Chamkha Ali J., Hashim Ishak (2018). Mixed convection of Al2O3-water nanofluid in a double lid-driven square cavity with a solid inner insert using Buongiorno's two-phase model, International journal of heat and mass transfer 119, 939-961.

Alsabery Ammar I., Ismael Muneer A., Chamkha Ali J., Hashim Ishak (2020). Effect of nonhomogeneous nanofluid model on transient natural convection in a non-Darcy porous cavity containing an inner solid body, International communications in heat and mass transfer 110, 104442.

Bhowmick Debayan, Randive Pitambar R., Pati Sukumar (2021). Implication of corrugation profile on thermo-hydraulic characteristics of Cu-water nanofluid flow through partially filled porous channel, International communications in heat and mass transfer 125,105329.

Chandra Sekhar Reddy R., Sudarsana Reddy P (2020). A comparative analysis of unsteady and steady Buongiorno's Williamson nanoliquid flow over a wedge with slip effects, Chinese journal of chemical engineering 28, 1767-1777.

Chen Hao, Guo Hang, Ye Fang, Fang Ma Chong (2021). A numerical study of orientated-type flow channels with porous-blocked baffles of proton exchange membrane fuel cells, International journal of hydrogen energy 46, 29443-29458.

Hoghoughi Gholamreza, Izadi Mohsen, Oztop Hakan F., Abu-Hamdeh Nidal (2018). Effect of geometrical parameters on natural convection in a porous undulant-wall enclosure saturated by a nanofluid using Buongiorno's model, Journal of Molecular Liquids 255, 148–159.

Hu Pengfei, Li Qi (2020). Effect of heat source on forced convection in a partially-filled porous channel under LTNE condition, International communications in heat and mass transfer 114, 104578.

Izadi Mohsen, Sinaei Sara, Mehryan S.A.M., Oztop Hakan., Abu-Hamdeh Nidal (2018). Natural convection of a nanofluid between two eccentric cylinders saturated by porous material: Buongiorno's two phase model, International journal of heat and mass transfer 127, 67-75.

Lakshmi K.M., Siddheshwar P.G., Laroze D (2020). Natural convection of water-copper nanoliquids confined in low porosity cylindrical annuli, Chinese journal of physics 68, 121-136.

Mahanthesha B., Shehzad S.A., Mackolil Joby, Shashikumar N.S. (2021). Heat transfer optimization of hybrid nanomaterial using modified Buongiorno model: A sensitivity analysis, International journal of heat and mass transfer 171, 121081.

Motlagh Saber Yekani, Soltanipour Hosseinali (2017). Natural convection of Al2O3-water nanofluid in an inclined cavity using Buongiorno's two-phase model, International journal of thermal sciences 111, 310-320.

Motlagh Saber Yekani, Taghizadeh Salar, Soltanipour Hosseinali (2016). Natural convection heat transfer in an inclined square enclosure filled with a porous medium saturated by nanofluid using Buongiorno's mathematical model, Advanced powder technology 27, 2526-2540.

Mustafa M. (2017). MHD nanofluid flow over a rotating disk with partial slip effects: Buongiorno model, International journal of heat and mass transfer 108, 1910-1916.

Oztop Hakan F (2006). Combined convection heat transfer in a porous lid-driven enclosure due to heater with finite length, International Communications in Heat and Mass Transfer, 772-779.

Sheikholeslami Mohsen, Rokni Houman B (2017). Effect of melting heat transfer on nanofluid flow in existence of magnetic field considering Buongiorno Model, Chinese journal of physics 55, 1115-1126.

Sheikhzadeh A., Nazari S. (2013). Numerical Study of Natural Convection in a Square Cavity Filled with a Porous Medium Saturated with Nanofluid, Transport Phenomena in Nano and Micro Scales 1, 138-146.

Sheremet M.A., Pop I., Rahman M.M. (2015). Three-dimensional natural convection in a porous enclosure filled with a nanofluid using Buongiorno's mathematical model, International journal of heat and mass transfer 82(2015 a)396-405.

Sheremet M.A., Pop I., Shenoy A. (2015b). Unsteady free convection in a porous open wavy cavity filled with a nanofluid using Buongiorno's mathematical model, International communications in heat and mass transfer 67, 66-72.

Sheremet M.A., Revnic C., Pop I (2017). Natural convective heat transfer through two entrapped triangular cavities filled with a nanofluid: Buongiorno's mathematical model, International journal of mechanical sciences 133, 484-494.

Sheremet Mikhail A., Pop Ioan (2018). Effect of local heater size and position on natural convection in a tilted nanofluid porous cavity using LTNE and Buongiorno's models, Journal of molecular liquids 266, 19-28.

Sheremet Mikhail A., Pop Ioan (2015). Free convection in a porous horizontal cylindrical annulus with a nanofluid using Buongiorno's model, Computers and fluids 118, 182-190.

Sheremet Mikhail A., Revnic Cornelia, Pop Ioan (2017). Free convection in a porous wavy cavity filled with a nanofluid using Buongiorno's mathematical model with thermal dispersion effect, Applied mathematics and computation 299, 1-15.

Tham Leony, Nazar Roslinda, Pop Ioan (2014). Mixed convection flow from a horizontal circular cylinder embedded in a porous medium filled by a nanofluid: Buongiorno Darcy model, International journal of thermal sciences 84, 21-33.

Lahlou Sara, Labsi Nabila, Benkahla Youb Khaled, Boudiaf Ahlem, Ouyahia Seif-Eddine (2020). Flow of viscoplastic fluids containing hybrid nanoparticles: Extended Buongiorno's model, Journal of non-Newtonian fluid mechanics 281, 104308.

Hussain Shafqat, Ahmed Sameh E (2019). Steady natural convection in open cavities filled with a porous medium utilizing Buongiorno's nanofluid model, International journal of mechanical sciences 157-158, 692-702.

Zhang Yingbo, Shen Chao, Zhang Chunxiao, Pu Jihong, Yang Qianru, Sun Cheng (2022). A novel porous channel to optimize the cooling performance of PV modules, Energy and built Environment 3, 210-225 .

Chu Yu-Ming, Ijaz Khan M., Khan Niaz B., Kadry Seifedine, Ullah Khan Sami, Tlilig Iskander, Nayak M.K. (2020). Significance of activation energy, bio-convection and magnetohydrodynamic in flow of third grade fluid (non-Newtonian) towards stretched surface: A Buongiorno model analysis, International communications in heat and mass transfer 118, 104893.